



A novel porous-carbon-based hollow fiber membrane with electrochemical reduction mediated by in-situ hydroxyl radical generation for fouling control and water treatment

Yue Yang, Sen Qiao*, Jiti Zhou, Xie Quan*

Key Laboratory of Industrial Ecology and Environmental Engineering (Ministry of Education, China), School of Environmental Science and Technology, Dalian University of Technology, Dalian 116024, PR China

ARTICLE INFO

Keywords:

Porous carbon
Hollow fiber membrane
Electro-Fenton
Hydroxyl radicals
Water treatment

ABSTRACT

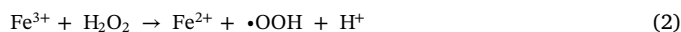
A novel process that combined hollow fiber membrane with electro-Fenton function was developed by bridging porous carbon (PC) with carbon nanotubes (CNTs) as the membrane materials. The cathode (PC-CNT hollow fiber membrane) reducing O_2 in-situ caused the rapid generation of H_2O_2 , and coupling with Fe^{2+} for the production of $\cdot OH$ as the main oxidant. The $\cdot OH$ could directly oxidize pollutants pass through the membranes, then, effluent quality was enhanced and membrane fouling was mitigated. Experimental results indicated that the removal efficiency of protein, glucose and phenol by PC-CNT hollow fiber membrane (optimized contents of CNT and PC was 1:1) at -0.8 V was about 2.7, 6.2 and 9.7 times higher than those of membrane separation alone, respectively. Experiments results demonstrated that PC-CNT hollow fiber membrane exhibited good stability by simultaneous filtration and electro-Fenton processing, demonstrating a great potential in membrane filtration system for effluent quality enhancement and membrane fouling control.

1. Introduction

As the global demand for freshwater continues to place significant pressure on available water resources, wastewater reclamation and reuse represent a viable water resource [1]. Membrane filtration was an efficient method in water treatment process due to its benefits of high effluent quality, simple process control, and compatibility to various types of wastewater [2–4]. Nevertheless, membrane fouling is a widespread problem in traditional membrane filtration process that generally leads to the deterioration of membrane performance, such as permeate flux loss [5]. Hence, the key to membrane fouling control is to completely prevent or greatly mitigate the deposition of various foulants on membrane surface [6]. Recently, many strategies with a view to mitigate the membrane fouling have been reported, like modifying membrane surface [7], improvement of module design [8], operation below the critical flux [9], relaxation and/or backwashing [10], and addition of chemicals [11].

A number of literatures have reported by employing the advanced oxidation processes (AOPs) as the way of fouling control in membrane filtration system [12–14]. The efficient production of active oxygen radicals played an important role in promoting advanced oxidation process [15]. Among divers reactive oxygen species, hydroxyl radical

($\cdot OH$) as one of the strong oxidizing agents, is able to unselectively react with the many contaminants. Especially, $\cdot OH$ radicals, consisting of a hydrogen atom bonded to an oxygen atom, easily steal hydrogen atoms from other molecules to form water molecules, which makes them highly reactive [16]. Hence, the supreme oxidation potential of $\cdot OH$ made it a strong oxidant in soil remediation, wastewater treatment, and also take part in plenty of physiological processes [17,18]. The most traditional method for generating $\cdot OH$ is by Fenton reaction, which has been studied for ~ 100 years [19]. In Fenton process, $\cdot OH$ production is greatly dependent on the efficient supply of H_2O_2 and Fe^{3+}/Fe^{2+} cycle as below:



Electro-Fenton is able to efficiently produce the H_2O_2 by two-electron reduction of dissolved oxygen on the cathode, thus avoiding the need of storage and transportation of H_2O_2 [19]. In addition, the effective cycle of Fe^{3+}/Fe^{2+} can be also accomplished by the electro-assistance. Among the electro-Fenton materials, porous carbon (PC) from the carbonization of metal organic framework was a promising electro-catalyzed material Benefiting from its high surface area and

* Corresponding authors.

E-mail addresses: qscyj@mail.dlut.edu.cn (S. Qiao), quanxie@dlut.edu.cn (X. Quan).

<https://doi.org/10.1016/j.apcatb.2019.117772>

Received 19 February 2019; Received in revised form 22 May 2019; Accepted 23 May 2019

Available online 25 May 2019

0926-3373/© 2019 Elsevier B.V. All rights reserved.

abundant pores, PC had abundant reactive sites and shortened transmission path for the electro-generation of H_2O_2 [20]. Under H_2 carbonization, PC was facily introduced the $\text{sp}^3\text{-C}$ and defects, which can serve as active sites to improve H_2O_2 selectivity under the electro-assistance [21–25].

From an engineering point of view, membrane fouling control in situ is greatly desirable however highly challenging. Fortunately, electro-Fenton has a high effectiveness for pollutants remove contrasted with the other electrochemical technologies, such as electrochemical repulsion and direct electrochemical oxidation [26–28]. $\cdot\text{OH}$ radicals are able to decompose the contaminants on membrane surface even inside membrane pores, thus effective mitigating membrane fouling. Herein, we propose a new high-flux membrane with in situ mitigation of membrane fouling by coupling electro-Fenton process. For the first time, CNTs bridging porous carbon-based (PC-CNT) hollow fiber membrane was developed and the anti-fouling mechanism was explored under the electro-assistance. Such a coupling process would offer at least two advantages: 1) $\cdot\text{OH}$ radicals and H_2O_2 could be effectively produced to mitigate in-situ the already deposited contaminants; 2) an electric field is able to be formed at the vicinity of cathode to restrain negatively contaminants deposition. The integrated system performance that couple the electro-Fenton process with the membrane filtration were comparatively evaluated by the mitigation of membrane fouling and the removal of natural organic pollutant, as well as illuminated how the membrane fouling was mitigated in the coupling system.

2. Results and discussion

2.1. Characterization of the PC-CNT hollow fiber membranes

After completely removing PVB via calcination in Ar flow at 800°C for 2 h, the PC/CNT/PVB hollow fibers transformed to free-standing PC-CNT hollow fiber membranes without any structural breakage (Fig. 1a and b). SEM images indicated that the obtained PC-CNT hollow fibers featured uniform outer/inner diameters ($850/500\ \mu\text{m}$) and crack-free surface without any pinholes. Meanwhile, the magnified surface in Fig. 1c presents the interwoven structures between PC and CNTs. Benefiting from high content of defects and $\text{sp}^3\text{-C}$, fast mass transfer and large surface area, PC was able to effectively generate H_2O_2 from O_2 reduction by electro-assistance [23]. CNTs exhibited encouraging electrical conductivity, which drew widespread attention in the field of electro-assisted membranes. Herein, a balance between PC and CNTs proportions played a significant role in the electro-assisted membrane separation process, because excess CNTs or PC amounts was adverse to the H_2O_2 productions or mechanical strength of membranes, respectively.

Fig. 1d–f shows SEM images of PC-CNT hollow fiber membranes with the different PC and CNTs proportions. It can be found that the PC contents increased with the increasing of PC/CNTs proportions from PC-CNT₁ to PC-CNT₃ hollow fiber membranes. The PC nanosheets were bridged by CNTs in favor of the stability of membrane structure. As shown in Fig. 1d, when the mass ratio of PC/CNTs was 1:2, the PC-CNT hollow fiber membrane exhibited a net structure interlaced by abundant CNTs, which was beneficial to increasing the porosity of membranes (Table S1). However, with the increasing of porous carbon contents, the plenty of two dimensional porous carbons were bridged by the CNTs, as shown in Fig. 1e. Meanwhile, the CNTs bridging the porous carbons were more obvious once the porous carbon contents were further increased shown in Fig. 1f. CNTs provided a unique one dimensional nanochannel for water transportation. The theoretical calculations indicated that the water permeation by a CNT was very fast [29,30]. Benefiting from its mass density and low resistivity, good chemical stability and large specific surface area, CNTs were acted as conduits for electron transporting [31,32]. Furthermore, because of the bridging of CNTs, the interlayer space between neighbored PC

nanosheets was expanded, which was favorable to the water flux. Therefore, the introduction of CNTs was beneficial for the water permeate flux and electrical conductivity of membranes. Fig. S2 presents the pore size distribution obtained from the PC-CNT hollow fiber membranes. The pore sizes of the PC-CNT₁, PC-CNT₂ and PC-CNT₃ hollow fiber membranes were 313, 153 and 104 nm, respectively, suggesting that the prepared PC-CNT hollow fiber membranes belonged to microfiltration membranes. Furthermore, the pore sizes of the PC-CNT hollow fiber membranes decreased with the increase of PC contents, indicating that the pore size can be controlled by adjusting the PC and CNTs contents.

As shown in Fig. S3, the prepared PC-CNT hollow fiber membranes possessed the good flexibility. The PC-CNT₂ hollow fiber membrane ($\sim 12\text{ cm}$ in length, Fig. S3a) could be bent into a semicircle and the curvature radius was about 2 cm without break (Fig. S3b–c). When the bent membrane was released, it can automatically and rapidly recover (Fig. S3d), suggesting it also featured structural rigidity. The structural rigidity was necessary for hollow fiber membranes to withstand pressure applied during filtration process. The typical stress–strain curve showed that the measured tensile strength was about 6 MPa for the PC-CNT₁ hollow fiber membrane (Fig. S4). However, the tensile strength decreased with the increasing of PC contents from PC-CNT₁ to PC-CNT₃ hollow fiber membranes, indicating that the increase of PC contents was disadvantage to the tensile strength of PC-CNT hollow fiber membranes. These excellent mechanical properties of PC-CNT hollow fiber membranes facilitated their assembly into a module and helped them withstand attacks from water flow in filtration process.

The introduction of CNTs not only promotes the mechanical properties, but also enhances the electric conductivity of PC-CNT hollow fiber membranes. To prove this hypothesis, the electrical characteristics of PC-CNT hollow fiber membranes were carried out by using a micromanipulator manual probe station [33]. As shown in Fig. S5, the $I - V$ plot of the PC-CNT₁, PC-CNT₂ and PC-CNT₃ hollow fiber membranes was a straight line that passed through the zero point. It was because of the increased CNTs content, leading to the disappearance of the interface barrier between porous carbons and the creation of a low-resistance ohmic contact between CNTs and PC. This indicated that the PC-CNT hollow fiber membranes possessed good electric conductivity, which was favorable to the electron transport. Meanwhile, it could be observed from Fig. S5 that the slope of $I - V$ plot from PC-CNT₁ to PC-CNT₃ hollow fiber membranes decreased with the increasing of porous carbon contents, reflecting that the electric conductivity of membranes decreased gradually. According to previous reports [23], porous carbons calcined at H_2 atmosphere had abundant $\text{sp}^3\text{-C}$ bonds and defects. Although these $\text{sp}^3\text{-C}$ bonds and defects were beneficial to the production of H_2O_2 , they were adverse to the electric conductivity of membranes.

Raman spectrum (Fig. S6) shows two peaks located at 1320 cm^{-1} (D band) and 1585 cm^{-1} (G band). The D band was associated with the introduction of $\text{sp}^3\text{-C}$ bonds and structure defects on the edges or basal plane, whereas the G band was related to graphitic carbon [23]. It could be found that the intensity ratios of D band to G band ($I_{\text{D}}/I_{\text{G}}$) of PC-CNT₁ hollow fiber membranes were less than 1.0, indicating that the $\text{sp}^2\text{-C}$ bonds accounted for the main part in PC-CNT₁ hollow fiber membranes. However, the values of $I_{\text{D}}/I_{\text{G}}$ were greater than 1.0 for the PC-CNT₂ and PC-CNT₃ hollow fiber membranes, which manifested that the $\text{sp}^3\text{-C}$ bonds and defects account for the main part in PC-CNT₂ and PC-CNT₃ hollow fiber membranes. It was reported that $\text{sp}^3\text{-C}$ bonds and defects of carbon nanomaterials can serve as active sites for the adsorption or reaction during the electrocatalytic process [23,34,35]. These characteristics of defects and $\text{sp}^3\text{-C}$ bonds were beneficial to the reduction of oxygen and thus facilitated H_2O_2 production.

Hydrophilia of membrane plays an important role in the membrane permeability. The novel PC-CNT₂ hollow fiber membrane retained the plentiful hydrophilic groups (Fig. S7, FTIR) on the surface, which endowed PC-CNT₂ hollow fiber membrane a good hydrophilia. Previous

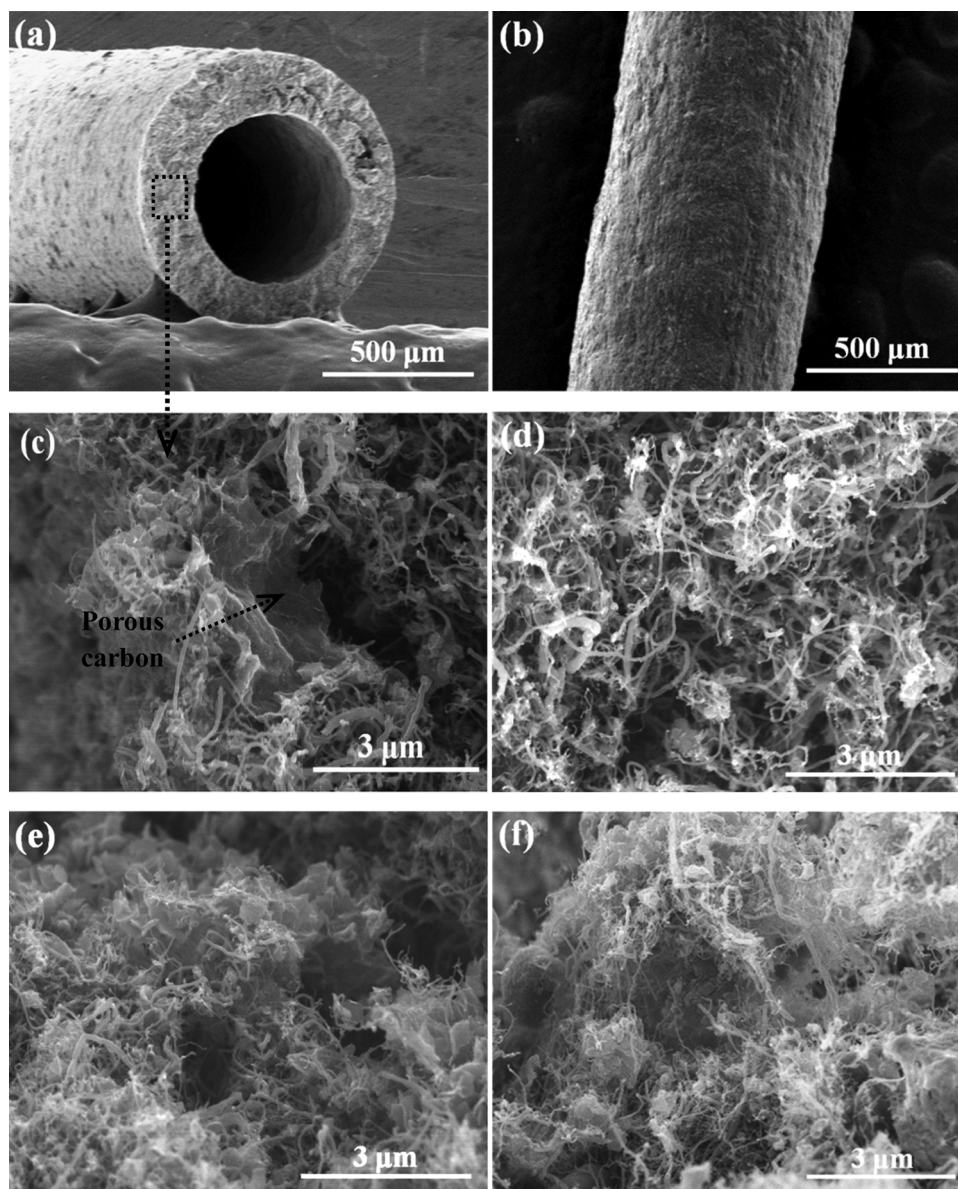


Fig. 1. SEM images of cross-section (a), profile (b) and magnified surface (c) of PC-CNT₂ hollow fiber membrane after thermal calcination at 800 °C for 2 h in Ar flow; SEM images of PC-CNT₁ (d), PC-CNT₂ (e) and PC-CNT₃ (f) hollow fiber membranes cross section with different PC and CNTs contents, respectively.

reports also found that electrochemistry could control the electrohydrodynamic behaviors of carbon materials, i.e., electrowetting and electrocapillarity [36–39]. Therefore, the water contact angle (WCA) of PC-CNT₂ hollow fiber membranes with and without electro-assistance was carried out. As shown in Fig. 2a, when the power source was turned on, a water droplet (2 μ L, 10 mM Na₂SO₄) displayed an initial WCA, and it completely spread out the hollow fiber membrane after \sim 2 s. However, when the same water droplet contacted the surface of PC-CNT hollow fiber membrane without electro-assistance, it took \sim 4.5 s for the water droplet to fully permeate into the membrane (Fig. 2b). These data suggested that our membrane featured strong hydrophilicity with electro-assistance, and the enhanced hydrophilicity had led to a shortened wetting time. The improved hydrophilicity under the electro-assistance was also beneficial to enhancing the filtration performance of PC-CNT₂ hollow fiber membrane. A hydrophilic surface can generate a water layer, which retarded the adsorption of protein, glucose and phenol.

The flux through the membrane increased linearly depending on pressure ranging from 0.01 to 0.05 MPa (Fig. 3c), suggesting the

structural stability of PC-CNT₂ hollow fiber membrane benefiting from the bridging of CNTs. As shown in Fig. 2c, the PC-CNT₂ hollow fiber membrane with the electro-assistance had a higher water flux than that of the same membrane in the absence of electro-assistance. This result could be explained that the electric potential applied in the membrane increased the electrohydrodynamic behaviors of carbon materials, which was consistent with the result of dynamic water contact angle (Fig. 2a and b). Fig. 2d showed that the water flux of the membranes increased gradually with the increasing of CNTs contents at same operating pressure. This phenomenon could be attributed to the ability of fast transmission of water through CNTs, meanwhile, the introduction of CNTs increased the porosity of membranes (Table S1). Hence, the high porosity and the hydrophilic performances of the hollow fiber membranes were the factors that led to a high flux of the PC-CNT hollow fiber membranes [40,41]. The permeability performances of different nanoparticles by the PC-CNT hollow fiber membrane were shown in Fig. 2e and f. For the PC-CNT₂ hollow fiber membrane, almost all the 5 nm Au nanoparticles were able to pass through the membrane, and only \sim 5% of them were retained on the feed side or inside the

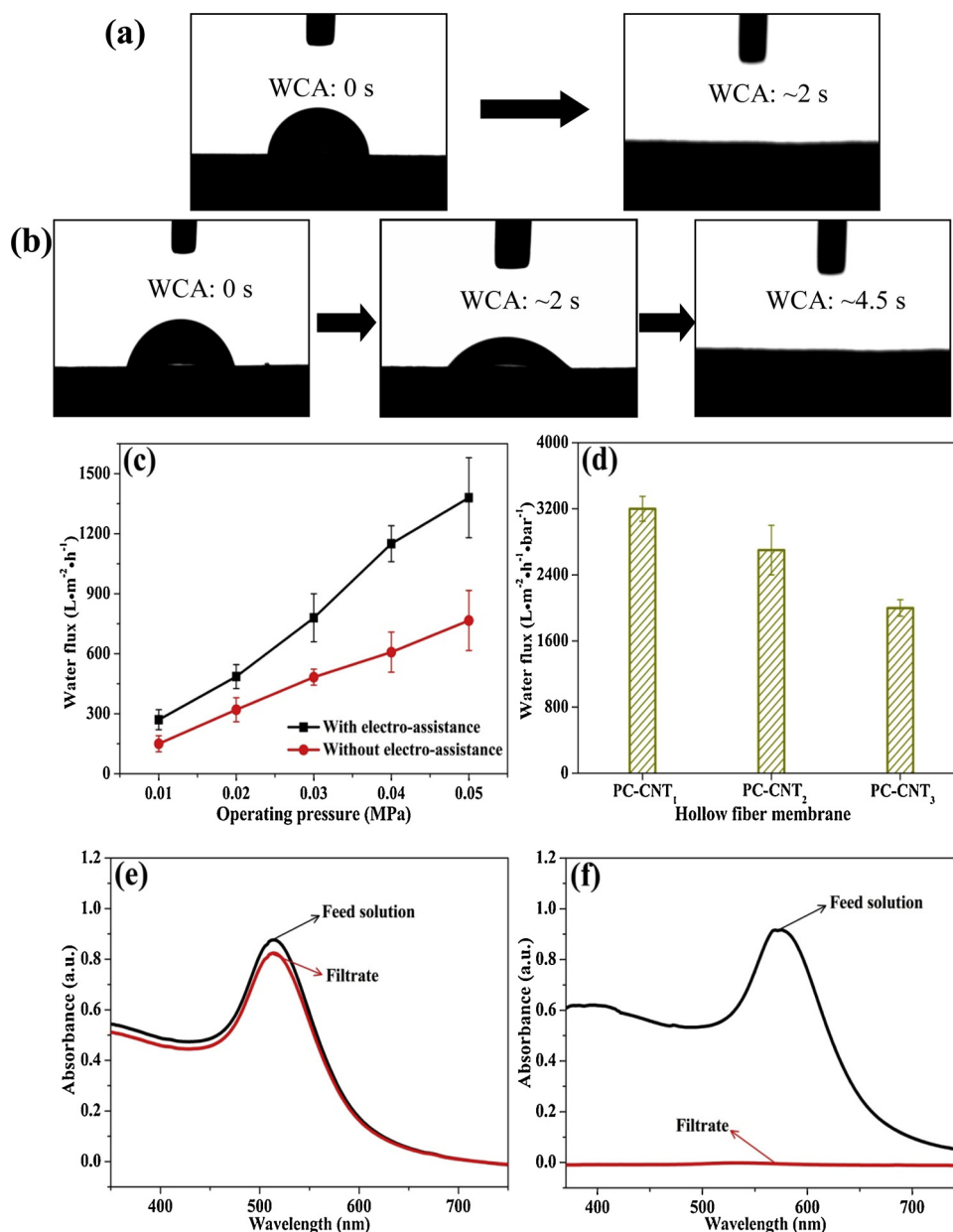


Fig. 2. Snapshots of dynamic water contact angle measurements on PC-CNT₂ hollow fiber membrane with (a) and without (b) electro-assistance; (c) Water flux change of PC-CNT₂ hollow fiber membrane with and without electro-assistance as a function of pressure; (d) Water flux of different PC-CNT hollow fiber membranes under electro-assistance; UV-vis spectra of different sizes of AuNPs dispersion before and after filtration using PC-CNT₂ hollow fiber membrane: (e) 5 nm and (f) 99 nm.

membranes (Fig. 2e). Compared to the filtration of 5 nm Au nanoparticles, all 99 nm Au nanoparticles were rejected, as shown in Fig. 2f.

2.2. Electrochemical generation of H₂O₂ on the surface of PC-CNT hollow fiber membranes

In our membrane separation process, the $\cdot\text{OH}$ was obtained from H₂O₂ decomposition by the electro-Fenton reaction based on Eqs (1 and 2) [42–44]. Therefore, the production of H₂O₂ played a vital role in the $\cdot\text{OH}$ production. The production of electro-generated H₂O₂ on PC-CNT hollow fiber membranes were investigated to visually evaluate the membrane performance. According to previous report,⁴¹ the bias voltage of H₂O₂ generation were selected at -0.6, -0.8 V and -1.0 V with pH of 3. As shown in Fig. 3b, when O₂ was electrochemically reduced on PC-CNT hollow fiber membrane, an optimal H₂O₂ production was obtained on PC-CNT₂ hollow fiber membrane from 21.5 to

40.0 $\mu\text{mol L}^{-1}$ at -0.6 to -1.0 V. However, under the same pH value, PC-CNT₁ and PC-CNT₃ hollow fiber membranes showed the relatively lower production of H₂O₂ at bias voltage from -0.6 to -1.0 V (Fig. 3a and c): 10.5–20.6 $\mu\text{mol L}^{-1}$ and 12.9–36.7 $\mu\text{mol L}^{-1}$ for PC-CNT₁ and PC-CNT₃ hollow fiber membrane, respectively. It suggested that a high production of H₂O₂ was obtained by PC-CNT₂ hollow fiber membrane even at a low bias voltage. H₂O₂ was generated by the electro-assisted porous carbons with the O₂, thus the production of H₂O₂ increased with the increasing of porous carbon contents. However, CNTs, as a good conductor of electricity, can efficiently transmit the electrons, which was beneficial for the H₂O₂ production. Both PC and CNTs contents played important roles in H₂O₂ production simultaneously. Based on previous experiments, the optimal H₂O₂ production was embodied on PC-CNT₂ hollow fiber membrane. In addition, Fig. 3b shows that the production of H₂O₂ at the applied voltage of -1.0 V was slightly higher compared with that of -0.8 V on PC-CNT₂ hollow fiber membrane.

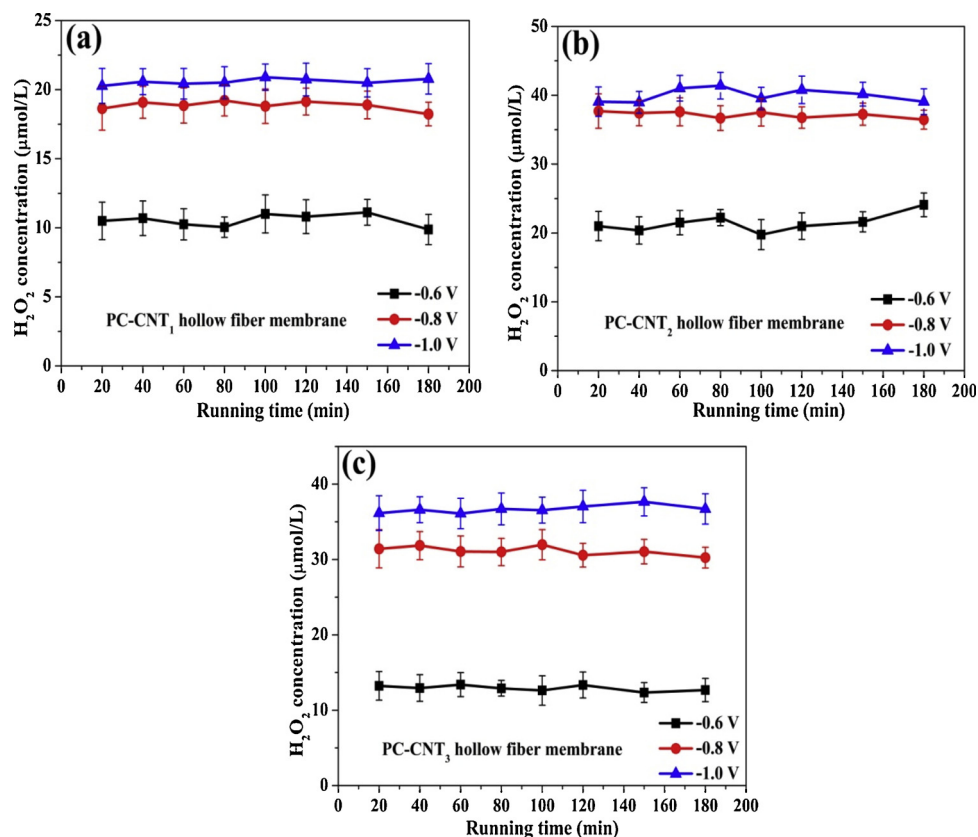


Fig. 3. H₂O₂ production rate at -0.6 V ~ -1.0 V over time with different PC-CNT hollow fiber membranes (a, PC-CNT₁; b, PC-CNT₂; c, PC-CNT₃).

Considering the energy savings, the following experiments were performed at -0.8 V.

2.3. Filtration and antifouling ability of PC-CNT hollow fiber membranes

Fouling resistance ability was crucial to the separation membrane applications in water treatment, since the severe fouling would reduce the permeation flux and shorten the membrane lifetime, which would lead to the increase of operating cost. The PC-CNT hollow fiber membrane was endowed with a good self-cleaning and anti-fouling properties because of $\cdot\text{OH}$ generation in situ. To investigate the regeneration capability of membranes, a bias voltage (-0.8 V) was applied on the PC-CNT₂ hollow fiber membrane and the humic acid (HA, 10 mg L⁻¹) was used as the target contaminant. As shown in Fig. 4a, the membrane in the absence of electro-assistance showed that the water flux went through a sharp drop when HA solution was filtrated into the hollow fiber membranes with time. However, a flux value of HA solution obviously increased when the power source was switched on. Meanwhile, the flux recovery by filtrating HA solution kept nearly constant by electro-assistance after each cycle. The scavenger experiments were carried out by adding tert-butyl alcohol to capture $\cdot\text{OH}$. The flux sharply declined after tert-butyl alcohol addition as shown in Fig. S8. These results demonstrated that coupling membrane separation of PC-CNT₂ with electro-assistance was advantageous for improving the recovery ability of the fouled membranes.

SEM images exhibited the PC-CNT₂ hollow fiber membrane after filtrating the HA without (Fig. 4b) and with (Fig. 4c) the electro-assistance, respectively. In the absence of the electro-assistance (Fig. 4b), the HA was heavily retained in the membrane surface with time. Hence, a thick contamination layer was observed on membrane surface without the electro-assistance compared to the membrane before filtration. However, the PC-CNT₂ hollow fiber membrane surface remained clean (Fig. 4c) as soon as the bias voltage was applied. The

above-mentioned results reflected that integrating the membrane with electro-Fenton was advantageous for enhancing the recovery ability of the fouled membrane. The phenomenon could be explained that the HA molecules retained on the membrane surface were degraded via the $\cdot\text{OH}$ from the Fe²⁺ and H₂O₂ (Fig. S8), thus achieving the membrane regeneration. Therefore, the electro-assisted PC-CNT₂ hollow fiber membrane had a good self-cleaning property. This self-cleaning property optimized the membrane cleaning operations and reduced the operating cost, offering chance for the application of PC-CNT₂ hollow fiber membrane in membrane filtration system.

The $\cdot\text{OH}$ generation process with H₂O₂ and Fe²⁺ on electro-assisted PC-CNT₂ hollow fiber membrane was carried out via tracing the intermediate species using the electron spin resonance (ESR) technique. As shown in Fig. 4d, a four-peak signal with an intensity ratio of 1:2:2:1 appeared on electro-assisted PC-CNT₂ hollow fiber membrane, which was similar to the typical spin adduct of $\cdot\text{OH}$ radicals [15]. Meanwhile, the typical peak signal did not appear on the PC-CNT₂ hollow fiber membrane without electro-assistance, suggesting that the $\cdot\text{OH}$ was produced under the electro-assistance. Furthermore, the DMPO- $\cdot\text{OH}$ adduct signals were also not found from the electro-assisted PC-CNT₂ hollow fiber membrane in the absence of Fe²⁺, indicating that H₂O₂ was incapable of being changed into the $\cdot\text{OH}$ radicals in the absence of Fe²⁺ ions.

To solve the issue of large membrane size rejecting the small size contaminants, electro-Fenton was coupled in the membrane filtration process [45–48]. Herein, the phenol was used for evaluating the removal ability of PC-CNT₂ hollow fiber membrane under the electro-Fenton assistance. Fig. 4e presents the time courses of the removal of phenol under different conditions. In the absence of electro-assistance, the PC-CNT₂ hollow fiber membrane showed a low phenol removal rate (8.6%). Because the phenol molecule was much smaller size than the membrane pore, phenol is not able to be removed only via size exclusion of the PC-CNT₂ hollow fiber membrane. At -0.8 V, about 83.5% of

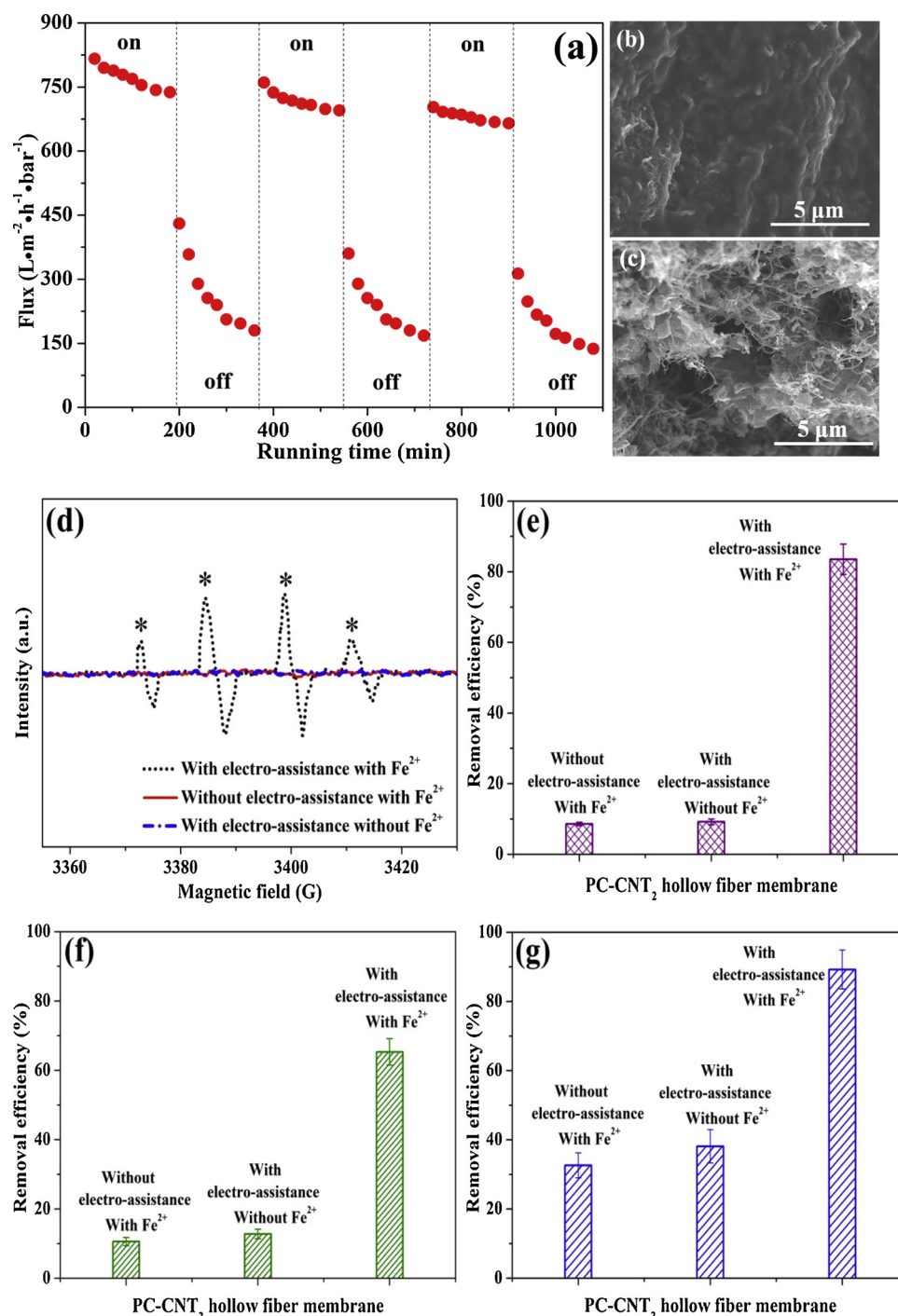


Fig. 4. (a) Recyclability of PC-CNT hollow fiber membrane with and without electro-assistance by removing HA; SEM images after filtrating the HA without (b) and with (c) the electro-assistance, respectively; (d) DMPO spin-trapping ESR spectra recorded under different conditions. Peaks generated from the DMPO–OH adducts are marked as (*); (e) Phenol, (f) glucose, and (g) protein removal efficiencies of PC-CNT₂ hollow fiber membrane with/without electro-assistance and without Fe^{2+} (operation time of 30 min).

phenol was removed by the PC-CNT₂ hollow fiber membrane with Fe^{2+} , which was approximately 9.7 times that of membrane filtration alone. The high removal rate of phenol for PC-CNT₂ hollow fiber membrane under the electro-assistance was mainly attributed to the efficient production of $\cdot\text{OH}$ by electro-Fenton on membrane surfaces. The removal of phenol using PC-CNT₂ hollow fiber membrane without Fe^{2+} was also performed under the electro-assistance for comparison. The removal rate of phenol was about 9.2%, which could be attributed to the adsorption effect of materials. The results were consistent with those of filtration ESP. Hence, the PC-CNT hollow fiber membrane

exhibited a good removal capability for phenol due to the electro-Fenton and filtration effect.

To evaluate the ability of the electro-assisted PC-CNT₂ hollow fiber membrane, the removal of glucose and protein was carried out. Fig. 4f shows the removal results of glucose for the PC-CNT₂ hollow fiber membrane. Approximately 65.4% of glucose was removed by the PC-CNT₂ hollow fiber membrane at -0.8 V with Fe^{2+} (0.4 mM), which was almost 6.2 times that of PC-CNT₂ hollow fiber membrane without the electro-assistance. Moreover, only 12.8% of glucose was removed by the electro-assisted PC-CNT₂ hollow fiber membrane without Fe^{2+} at

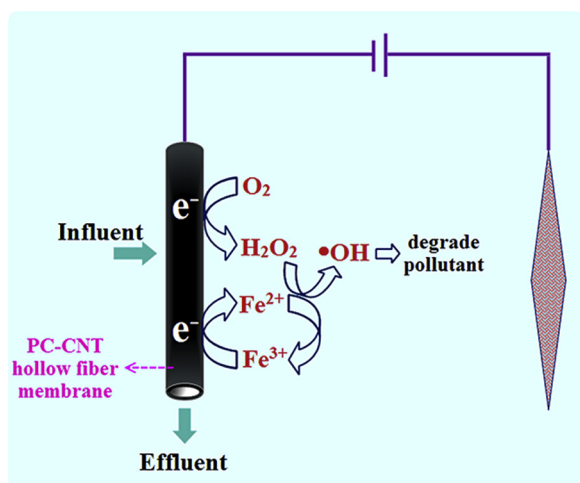


Fig. 5. Conceptual illustration of the electro-Fenton assisted PC-CNT₂ hollow fiber membrane for fouling suppression by using in-situ generated $\cdot\text{OH}$.

the same voltage, however this value was much lower compared with PC-CNT₂ hollow fiber membrane with the electro-assistance and Fe^{2+} . The enhanced removal rate for the electro-assisted presence was due to the synergistic effect of filtration and electro-Fenton. Fig. 4g presents the removal of protein using the PC-CNT₂ hollow fiber membrane with different conditions. It can be found that the removal efficiency of protein was about 89.2% by the electro-assisted PC-CNT₂ hollow fiber membrane with Fe^{2+} , which was approximately 2.7 and 2.3 times higher compared with the PC-CNT₂ hollow fiber membrane in the absence of electro-assistance and electro-assisted PC-CNT₂ hollow fiber membrane without Fe^{2+} , respectively. Moreover, it can be also found from the inset of Fig. S9a that the PC-CNT₂ hollow fiber membrane had a clean surface similar to that of original PC-CNT₂ hollow fiber membrane. However, the PC-CNT₂ hollow fiber membrane without the electro-assistance or Fe^{2+} showed a contaminated membrane surface (Fig. S9b and c). These results indicated that the introduction of electro-Fenton was beneficial to alleviating the membrane fouling.

In order to investigate the stability and reusability of the PC-CNT₂ hollow fiber membrane, the cyclic coinstantaneous filtration and electro-Fenton was carried out. As displayed in Fig. S10, the PC-CNT₂ hollow fiber membrane kept a high phenol removal efficiency (~80%) even after the four cycles. This result implied that the PC-CNT₂ hollow fiber membrane had a good stability at long-term operation process, which can be due to the outstanding scavenging activity of $\cdot\text{OH}$ radicals.

Herein, we summarized a mechanism of electrochemistry enhancing the water flux and pollutant removal. For the high water flux, electrochemistry could control the electrohydrodynamic behaviors of carbon materials, like electrowetting and electrocapillarity [48]. Fig. 2 shows that the hydrophilicity of PC-CNT₂ hollow fiber membrane was enhanced under the electro-assistance. The improved hydrophilicity also contributed to the enhanced water permeation flux of PC-CNT₂ hollow fiber membrane under the electro-assistance. The mechanism of enhanced pollutant removal depended on the strong oxidation capacity of $\cdot\text{OH}$ radicals from electro-Fenton process. As shown in Fig. 5, H_2O_2 was generated by the reduction of O_2 under the electro-assistance, and subsequently, H_2O_2 coupling with Fe^{2+} produced the $\cdot\text{OH}$ radicals. The $\cdot\text{OH}$ radicals were utilized to degrade the pollutant and Fe^{3+} was reduced into Fe^{2+} with electro-assistance. Thus the $\text{Fe}^{2+}/\text{Fe}^{3+}$ realized the efficient circulation.

Notes

The authors declare no competing financial interests.

Acknowledgements

This work was financial supported by the National Natural Science Foundation of China (No. 21677026), the LiaoNing Revitalization Talents Program (No.XLYC1807067), the Fundamental Research Funds for the Central Universities (DUT17LAB15), and the Programme of Introducing Talents of Discipline to Universities (B13012).

Appendix A. Supplementary data

Supplementary material related to this article can be found, in the online version, at doi:<https://doi.org/10.1016/j.apcatb.2019.117772>.

References

- [1] K.P. Katuri, C.M. Werner, R.J. Jimenez-Sandoval, W. Chen, S. Jeon, B.E. Logan, Z.P. Lai, G.L. Arny, P.E. Saikaly, Environ. Sci. Technol. 48 (2014) 12833–12841.
- [2] C.M. Chung, T. Tobino, K. Cho, K. Yamamoto, Water Res. 96 (2016) 52–61.
- [3] X. Zheng, Y.F. Zhou, S.H. Chen, H. Zheng, C.X. Zhou, Desalination 250 (2010) 609–612.
- [4] A. Santos, W. Ma, S.J. Judd, Desalination 273 (2011) 148–154.
- [5] P. Blanpain-Avet, J.F. Migdal, T. Benezech, J. Membr. Sci. 337 (2009) 153–174.
- [6] Y. Yang, S. Qiao, R.F. Jin, J.T. Zhou, X. Quan, Water Res. 151 (2019) 54–63.
- [7] J. Zhou, W. Li, J.S. Gu, H.Y. Yu, Membr. Water Treat. 1 (2010) 83–92.
- [8] F.I. Hai, K. Yamamoto, K. Fukushi, Desalination 199 (2006) 305–307.
- [9] B.D. Cho, A.G. Fane, J. Membr. Sci. 209 (2002) 391–403.
- [10] J.L. Wu, P. Le-Clech, R.M. Stuetz, A.G. Fane, V. Chen, J. Membr. Sci. 324 (2008) 26–32.
- [11] H. Koseoglu, N.O. Yigit, V. Iversen, A. Drews, M. Kitis, B. Lesjean, M. Kraume, J. Membr. Sci. 320 (2008) 57–64.
- [12] H.C. Lan, W.J. He, A.M. Wang, R.P. Liu, H.J. Liu, J.H. Qu, C.P. Huang, Water Res. 105 (2016) 575–582.
- [13] P.Y. Liang, M. Rivallin, S. Cerneaux, S. Lacour, E. Petit, M. Cretin, J. Membr. Sci. 510 (2016) 182–190.
- [14] S.A. Neto, A.R. de Andrade, Electrochim. Acta 54 (2009) 2039–2045.
- [15] Y.X. Li, S.X. Ouyang, H. Xu, X. Wang, Y.P. Bi, Y.F. Zhang, J.H. Ye, J. Am. Chem. Soc. 138 (2016) 13289–13297.
- [16] S. Gligorovski, R. Strekowski, S. Barbati, D. Vione, Chem. Rev. 115 (2015) 13051–13092.
- [17] X. Yang, X. Xu, J. Xu, Y. Han, J. Am. Chem. Soc. 135 (2013) 16058–16061.
- [18] M.A. Voinov, J.O.S. Pagán, E. Morrison, T.I. Smirnova, A.I. Smirnov, J. Am. Chem. Soc. 133 (2011) 35–41.
- [19] H. Li, J. Shang, Z.P. Yang, W.J. Shen, Z.H. Ai, L.Z. Zhang, Environ. Sci. Technol. 51 (2017) 5685–5694.
- [20] J.K. Sun, Q. Xu, Energy Environ. Sci. 7 (2014) 2071–2100.
- [21] J.B. Jia, D. Kato, R. Kurita, Y. Sato, K. Maruyama, K. Suzuki, S. Hirono, T. Ando, O. Niwa, Anal. Chem. 79 (2007) 98–105.
- [22] J.C. Byers, A.G. Guell, P.R. Unwin, J. Am. Chem. Soc. 136 (2014) 11252–11255.
- [23] Y.M. Liu, X. Quan, X.F. Fan, H. Wang, S. Chen, Angew. Chem. Int. Ed. 54 (2015) 6837–6841.
- [24] B.P. Chaplin, Environ. Sci. Proc. Imp. 16 (2014) 1182–1203.
- [25] W.L. Jiang, X. Xia, J.L. Han, Y.C. Ding, M.R. Haider, A.J. Wang, Environ. Sci. Technol. 52 (2018) 9972–9982.
- [26] Y. Yang, S. Qiao, R.F. Jin, J.T. Zhou, X. Quan, J. Membrane Sci. 553 (2018) 54–62.
- [27] Y. Yang, S. Qiao, R.F. Jin, J.T. Zhou, X. Quan, Environ. Sci. Technol. 53 (2018) 1014–1021.
- [28] X.F. Fan, Y.M. Liu, X. Quan, S. Chen, Environ. Sci. Technol. 52 (2018) 1444–1452.
- [29] G. Hummer, J.C. Rasaiah, J.P. Noworyta, Nature 414 (2001) 188–190.
- [30] K. Falk, F. Sedlmeier, L. Joly, R.R. Netz, L. Bocquet, Nano Lett. 10 (2010) 4067–4073.
- [31] I. Robel, B.A. Bunker, P.V. Kamat, Adv. Mater. 17 (2005) 2458–2463.
- [32] A. Kongkanand, P.V. Kamat, ACS Nano 1 (2007) 13–21.
- [33] H. Wang, X. Quan, H. Yu, S. Chen, Carbon 46 (2008) 1126–1132.
- [34] A. Ueda, D. Kato, N. Sekioka, T. Kamata, R. Kurita, H. Uetsuka, Y. Hattori, S. Hirono, S. Umemura, O. Niwa, Carbon 47 (2009) 1943–1952.
- [35] G. Zhong, H. Wang, H. Yu, F. Peng, Electrochem. Commun. 40 (2014) 5–8.
- [36] I. Masselin, L. Durand-Bourlier, J.M. Laine, P.Y. Sizaret, X. Chasseray, D. Lemordant, J. Membr. Sci. 186 (2001) 85–96.
- [37] W. Sun, T. Chen, C. Chen, J. Li, J. Membr. Sci. 305 (2007) 93–102.
- [38] L. Wang, X. Wang, J. Membr. Sci. 283 (2006) 109–115.
- [39] Z. Wang, L. Ci, L. Chen, S. Nayak, P.M. Ajayan, N. Koratkar, Nano Lett. 7 (2007) 697–702.
- [40] S. Kaur, R. Gopal, W.J. Ng, S. Ramakrishna, T. Matsuura, MRS Bull. 33 (2008) 21–26.
- [41] R.S. Barbate, S. Sundararajan, D. Pliszka, S. Ramakrishna, Filtr. Sep. 45 (2008) 32–35.
- [42] E. Brillas, I. Sirés, M.A. Oturan, Chem. Rev. 109 (2009) 6570–6631.
- [43] J.J. Pignatello, E. Oliveros, Crit. Rev. Macromol. Sci. Technol. 36 (2006) 1–84.
- [44] Y.M. Liu, S. Chen, X. Quan, H.T. Yu, H.M. Zhao, Y.B. Zhang, Environ. Sci. Technol. 49 (2015) 13528–13533.
- [45] M.M. Pendergast, E.M.V. Hoek, Energy Environ. Sci. 4 (2011) 1946–1971.
- [46] Y.J. Won, J. Lee, D.C. Choi, H.R. Chae, I. Kim, C.H. Lee, I.C. Kim, Environ. Sci. Technol. 46 (2012) 11021–11027.
- [47] M.E. Warkiani, A.A.S. Bhagat, B.L. Khoo, J. Han, C.T. Lim, H.Q. Gong, A.G. Fane, ACS Nano 7 (2013) 1882–1904.
- [48] X.F. Fan, H.M. Zhao, Y.M. Liu, X. Quan, H.T. Yu, S. Chen, Environ. Sci. Technol. 49 (2015) 2293–2300.